Texture control of $PbTiO_3$ and $Pb(Zr,Ti)O_3$ thin films with TiO_2 seeding

P. Muralt, T. Maeder, L. Sagalowicz, and S. Hiboux

Laboratoire de Céramique, Ecole Polytechnique Fédérale de Lausanne, CH-1015 Lausanne, Switzerland

S. Scalese, D. Naumovic, and R. G. Agostino

Institut de physique, Université de Fribourg, CH-1700 Fribourg, Switzerland

N. Xanthopoulos and H. J. Mathieu

Laboratoire de Me´tallurgie Chimique, Ecole Polytechnique Fédérale de Lausanne, CH-1015 Lausanne, Switzerland

L. Patthey and E. L. Bullock

Institut de Physique Experimentale, Université de Lausanne, CH-1015 Lausanne-Dorigny, Switzerland

Version of record: Journal of Applied Physics 83 (7), 3835-3841, 1998.
http://hdl.handle.net/10.1063/1.366614

Abstract

The nature and the role of 1 to 5 nm thick TiO_2 seed layers for the growth of textured $PbTiO_3$ and $Pb(Zr,Ti)O_3$ thin films on textured Pt(111) thin film substrates have been studied. Under otherwise identical *in situ* sputter deposition process conditions, the $PbTiO_3$ texture could be turned from (100) to (111) orientation by adding the seed layer. This is demonstrated by patterning the TiO_2 film. Auger electron spectroscopy and x-ray photoemission spectroscopy showed that the seed layer was a continuous TiO_2 film. X-ray photoelectron diffraction measurements revealed epitaxial ordering in the seed layer. As there is no azimuthal order among the Pt grains, the reduced information of azimuthally averaged polar cuts is obtained. These give strong evidence for a strained rutile (110) structure. Various deposition experiments indicated that the TiO_2 is effective only when it is ordered before the $PbTiO_3$ nucleation starts. The epitaxial relationship between $PbTiO_3$ (111) and Pt(111) is thus mediated by the intermediate, epitaxial TiO_2 film, which is dissolved or transformed to $PbTiO_3$ afterwards. The observed growth behavior is discussed in terms of surface and interface energies.

1 Introduction

Ferroelectric thin films of the $PbZr_xTi_{1-x}O_3$ ($0 \le x \le 0.7$) (PZT) solid solution system have important applications in memory and microelectro-mechanical devices. For these applications it is required that they are integrated on silicon substrates. Unfortunately, it is not possible to grow PZT directly on silicon [1], because of interfacial chemical reactions and Pb – Si interdiffusion during deposition in strongly oxidizing conditions and at elevated temperatures between 550 and 700 °C. A number of buffer, barrier and adhesion layers need to be introduced, be it electrically insulating oxide films such as SiO_2 [2], or conductive oxide barrier systems based on RuO_2, for instance [3]. Epitaxial relationships down to the silicon substrate can be obtained but with a large effort [4]. However, for most applications, a high degree of film texture would be sufficient. This is most obvious for pyroelectric devices which only require the highest possible degree of polarization perpendicular to the film plane. In other applications, the ability to control the film texture is very desirable for the study of properties, and later for optimization of properties and reproducibility.

PZT does not exhibit dominant self texture growth mechanisms, as, e.g., occur in the layered perovskite $Bi_4Ti_3O_{12}$ [4]. Nucleation, and therefore also texture, are mainly governed by the underlying substrate and the interface properties. Additionally, surface energies of PZT and the ion diffusivity of its constituents are expected to play a role. The standard substrate is a platinum film, as for most applications PZT has to be

grown on a bottom electrode. The complete electrode system commonly used is $Pt/Ti/SiO_2/Si$ [2]. Pt is chosen for its chemical inertness and its relatively low diffusivity, and Ti serves as an adhesion layer. The growth of PZT is nucleation controlled [5]. It is therefore possible to promote the nucleation by suitable electrodes as substrates, and thus to obtain a textured, columnar growth. At first glance, platinum looks like an ideal substrate. Its lattice constant (3.92 Å at room temperature) matches by 0.5% the one of $PbTiO_3$ and by 4% the one of PZT50/50 (x=0.5) at the growth temperatures. As platinum can be grown with a high degree of (111) texture, a (111) orientation of PZT is expected to be favored. It is usually found, however, that many different orientations can be obtained on Pt (111) [6]. In addition, it was shown by Aoki *et al.* [7] that pure platinum is not the ideal substrate to nucleate the perovskite. A low nucleation density, and consequently, high leakage currents have been observed. The same authors recognized that Ti plays a key role in the nucleation of the perovskite phase. A few nanometer thick layer of Ti on the platinum was sufficient to obtain a high nucleation density resulting in a dense film, which exhibited much lower leakage currents. This role of Ti is masked when using the standard Pt/Ti electrodes, because the Ti is supplied unintentionally by the adhesion layer, which partially diffuses up to the Pt surface [2,8]. For this reason, standard Pt/Ti electrodes improve with suitable tempering procedures before deposition [9,10]. It can be assumed that they provide a certain amount of titanium oxide (i.e., titania) on the surface.

The chemical effect of a Ti-rich layer at the PZT/Pt interface manifests itself in a lowering of the nucleation temperature, since Ti-rich PZT exhibits a lower activation energy for nucleation [5]. In addition, there also exists a physical effect which makes the above mentioned nanometer thick Ti films work as a seed layer for (111) oriented growth of PZT [7]. We have observed the same behavior for nanometer thick TiO_2 films, when studying the initialization of the growth of $PbTiO_3$ by *in situ* reactive sputtering from a lead and a titanium source [11]. The seeding of the orientation works only with 1 to 5 nm thin Ti [7] or TiO_2 films. It can be assumed that for both the same mechanism applies, and that the Ti is oxidized to TiO_2 prior to PZT crystallization.

To date, no explanation for the orientational effects of TiO_2 seeding has been given. The goal of this paper is to gain more insight into this phenomenon. Nanometer thick TiO_2 films on Pt (111) have been investigated in detail and their impact on film texture of sputter deposited $PbTiO_3$ and PZT has been studied. The results presented below are not restricted to sputter deposition alone. It turned out that such titania seed layers almost inevitably lead to a (111) texture, also when sol-gel deposition techniques are applied. The influence of the seed layer is stronger than that of process parameters such as pyrolysis and annealing temperature, heating rates, and lead excess, which usually are the parameters optimized for orientation control [6]. This seed layer already has been successfully applied for the fabrication of pyroelectric devices [12].

2 Experiments and results

Platinum films were grown by sputter deposition at 400°C substrate temperature on Ta or TiO_2 adhesion layers onto thermally oxidized silicon wafers. The processes have been optimized for obtaining highly textured (111) platinum films, as measured by x-ray θ-2θ diffraction scans, and verified by pole figures. For the platinum film, the Ta and Ti adhesion layers play the role of texture seeding, as is also reported for other systems like Al and Cu on Ti and TiN [13].

Both adhesion layers do not diffuse to the top of the Pt during later processing, as was verified by means of Auger electron spectroscopy. There is thus no unintentional Ti present on the Pt, which could falsify the experiment when testing the bare platinum electrode. Next, the 0 to 10 nm thick TiO_2 overlay, followed by the *in situ* deposited $PbTiO_3$ or PZT have been grown at 530 to 570°C. This process applies two or three simultaneously operating magnetrons which are passed over periodically by the substrate holder, depositing roughly one monolayer per turn (see Refs. [14] and [15] for details). It did not matter whether the vacuum was broken in-between the TiO_2 and $PbTiO_3$ depositions. Transmission electron microscope (TEM) analysis of the PZT films showed no traces of the less than 3 nm thick TiO_2 layers. It can be concluded that the titania layer reacts with excess lead and transforms to $PbTiO_3$. This is in accordance with earlier observations that up to 10 monolayers of TiO_2 react in a few seconds with the incoming PbO flux in order to form the perovskite [15].

An x-ray study was performed in order to determine the optimal seed layer thickness. With no TiO_2 overlay, (100)-oriented perovskite was obtained at high lead oxide fluxes (more than twice the TiO_2 flux), pyrochlore was obtained at low lead oxide fluxes. In between there is a transition zone of randomly oriented perovskite. When a TiO_2 seed layer was added, the (111) orientation appeared predominantly, independent of the lead flux. θ-2θ diffraction scans yielded an optimal TiO_2 film thickness between 1 and 2 nm for obtaining the (111) texture. This was not only found for $PbTiO_3$, but also for PZT with up to 60% Zr. Figure 1 shows the weighted relative intensities of (100), (110), and (111) θ-2θ diffraction peaks obtained with PZT 45/55 as a function of seed layer thickness. It shows that an almost complete (111) orientation of the diffracting grains is obtained. The texture quality was verified by means of pole figures, because the absence of peaks of other orientations in the θ-2θ diffraction scan is only a necessary, yet not sufficient condition for a high degree of texture [13]. Figure 2 shows the (111) peak as a function of the substrate tilt angle. The small line width with half signal tilt ω_{50} (see Ref. [13]) of 2° to 3° proves that a very good texture was indeed obtained. Comparison to quantitative analysis performed in Ref. [15] with Al (111) films indicates that less than 10% of the grains are randomly oriented.

An illustrative demonstration of such a seed layer based texture control was obtained by patterning the TiO_2 seed layer (70 μm wide lines with 30 μm wide spacings). This was executed by standard photolithography and etching in a CF_4 plasma. The 100 nm thick $PbTiO_3$ film grown on top showed clearly an image of the mask (see Fig. 3), observed with both optical and scanning electron microscopy (SEM). Two reference samples (with and without titania) served to identify the orientations by means of SEM images. The parts covered with titania exhibited the (111) orientation and a small grain size, which was about the same as the one of the underlying Pt film (typically 100 to 300 nm). In contrast, the parts without TiO_2 showed much larger grains covering several grains of platinum. Additionally, a surface corrugation due to a dense domain structure is well visible. The regions with (111) orientation exhibit a slightly thicker film (see Fig. 4). The 5 nm difference can mainly be attributed to the reaction of the 2 nm thick TiO_2 with excess lead. Both textures thus yield the same growth rate. The latter is defined by the TiO_2 flux only, since excess lead is re-evaporated.

It has to be noted that for both orientations a well textured Pt (111) substrate is necessary. In both cases we thus deal with epitaxial relationships to Pt (111) surfaces. In the case of the (100) orientation this fact is also supported by the occurrence of 120° angles between domain features. The tetragonal structure allow only angles of 90° and 180° between the ferroelectric domains. Hence, 120° angles must originate from epitaxy of two grains starting on the same platinum (111) grain, and copying two different unit cell directions from the hexagonal surface symmetry. The (110) axis of the (001) perovskite matches best along one of the 3 directions of shortest Pt–Pt distances: [1,-1,0], [1,0,-1] and [0,1,-1].

For a better understanding of the ‘‘epitaxial glue’’ electrodes with TiO_2 seed layers have been characterized by Auger electron spectroscopy (AES), x-ray photoelectron spectroscopy (XPS), and x-ray photoelectron diffraction (XPD [16,17]). The XPS Ti 2*p* peak was found at 458.6 eV (C 1*s* at 285.0 eV), confirming the chemical composition of the TiO_2. Auger spectroscopy combined with 2 keV Ar^+ depth profiling showed that the surface was completely (2 nm) or almost completely (1 nm) covered by the seed layers (Fig. 5). In addition, depth profiling confirmed the thicknesses obtained by the power times time regulation of the sputter process. These results prove that the $PbTiO_3$ films started indeed to nucleate on a continuous TiO_2 layer.

We further investigated whether this TiO_2 layer itself was ordered, having an epitaxial relationship to the underlying platinum, or whether it was amorphous. The first possibility was suggested by the finding that no (111) orientation in sol-gel deposited films was obtained when depositing the TiO_2 film at room temperature, while hot deposited TiO_2 or post-annealed TiO_2 yielded always a (111) orientation. For reasons of chemical selectivity, XPD was considered to be the best technique to detect any order in such a thin film. In the given case of a textured film, no dependence on the azimuthal angle is observed, resulting in ring patterns in the full two-dimensional scan image. The values have been therefore averaged over the azimuthal angle (azimuthally averaged polar cut). The Pt 4*f* photoelectron diffraction measurements of the uncoated, as well as of the coated platinum films showed a good correspondence with the azimuthally averaged polar cut of a single crystal reference sample (see Fig. 6). The surfaces of the platinum grains of the polycrystalline film are thus well (111)-oriented, confirming the x-ray diffraction data.

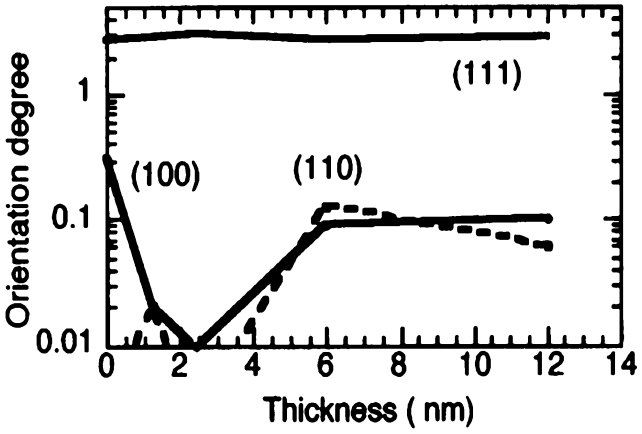

Figure 1. Film texture of 300 nm thick PZT 45/55 films deposited at 570°, as evaluated by means of θ-2θ xray diffraction scans. The degree of orientation is calculated from the (100), (110), and (111) peak intensities, which are weighed by the corresponding powder diffraction intensities. Sum and maximum value are 3.

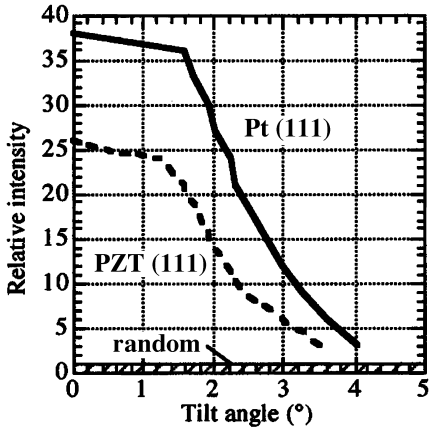

Figure 2. Cross section trough pole figure plot of a 0.9 µm thick PZT 45/55 film on Pt/TiO_2/Ti electrodes measured on a PW1830 Philips system, showing the intensity of the (111) x-ray diffraction peak as a function of the substrate tilt angle. The signal is given relative to the averaged intensity corresponding to random orientation.

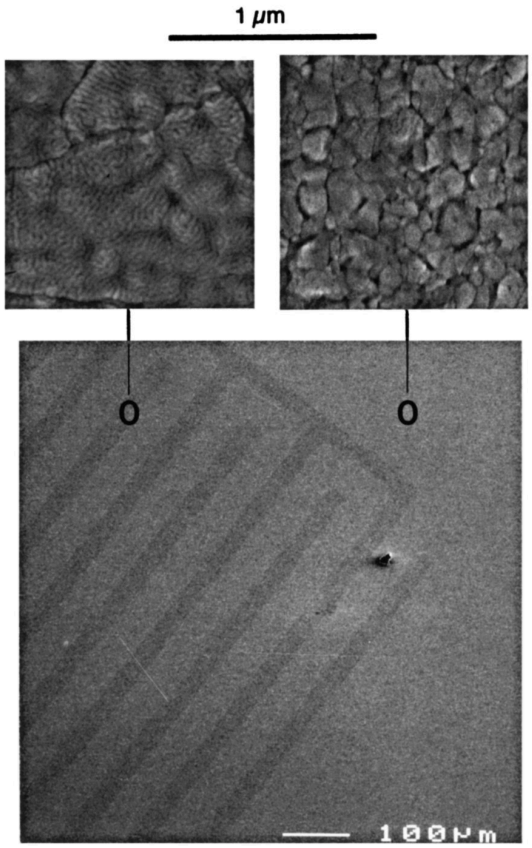

Figure 3. SEM photograph of a $PbTiO_3$ film above a patterned TiO_2 seed layer. At the 30 µm wide darker regions the TiO2 has been removed.

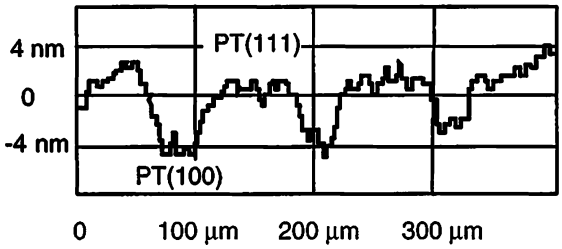

Figure 4. Profilometric scan over the surface of the $PbTiO_3$ orientation pat- tern. A corrugation amplitude of 4 to 6 nm can clearly be seen.

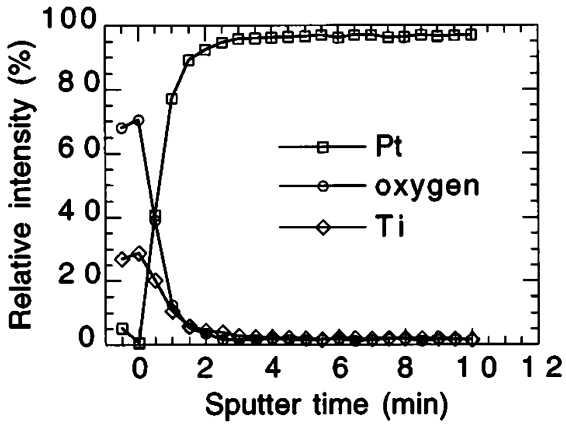

Figure 5. Auger depth profile through the 1 nm TiO_2 film on the platinum layer for the elements Ti, O, Pt. The sputter etching rate was 0.7 nm/min.

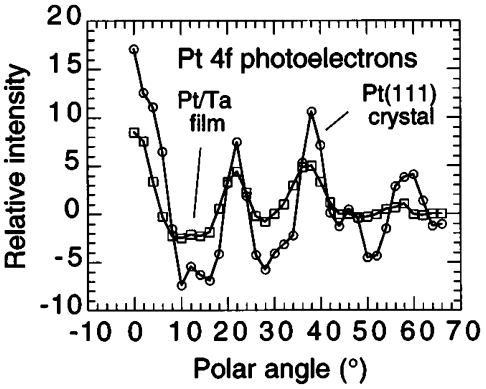

Figure 6. Average polar XPD cut from Pt 4*f* photoelectrons obtained with a Si *Kα* source. The Pt (111) thin film is compared with the Pt (111) single crystal. The signal is given in of the background signal.

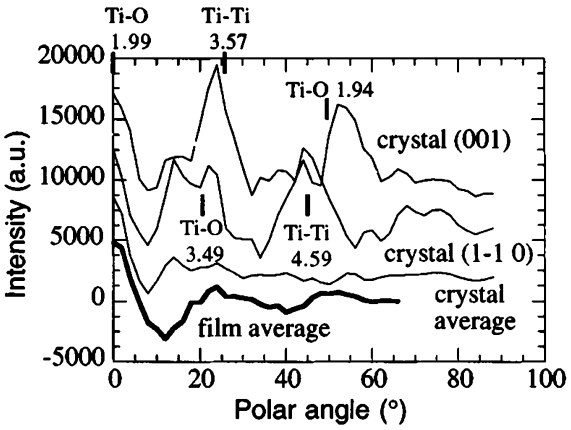

Figure 7. Polar cuts of XPD scans from Ti 2*p* photoelectrons. The fat solid curve is the azimuthally averaged scan of the TiO_2 thin film (Si *Kα* source, 1281 eV). Three polar cuts of the (110) rutile single crystal are shown for comparison (Al *Kα* source, 954 eV): the polar cuts of the [0,0,1] and the [-1,1,0] directions, and the one obtained by averaging over the azimuthal angle. The background has been subtracted. The intensity of the thin film does not scale with the other intensities. The polar angles of the most important bonds are marked by strokes.

The Ti 2*p* photoelectron diffraction finally revealed that also the 1 nm thick TiO_2 seed layer was textured (Fig. 7). It is known that the XPD intensity peaks at the directions of nearest neighbor bonds at high enough energies (> 500 eV). In the spectra of XPD measurements on (110) facets of rutile single crystals, the main peaks of the two-dimensional scan can be identified with special Ti-Ti or Ti-O bond direction [18,19]. High intensities are obtained in direction of near neighboring atoms and along lines of a high density of atoms, thus along important axes.

With the reduced information of the average polar cut it is not possible to deduce the structure of the film. But we can check, which surface among the low index facets of rutile and anatase is most compatible. Best coincidence is obtained with rutile (110), for which the second shortest Ti–O bond (1.99 Å) points along [110], yielding the strong peak at the polar angle $\theta = 0°$, and the second shortest Ti–Ti bond (3.6 Å) points along [1/2,1/2,1/2], yielding the other strong peak at $\theta = 24.5°$ in the single crystal (see Table I and Fig. 6, cut [001]). This peak is also well maintained in the azimuthally averaged polar scan derived from single crystal measurements. The strong peak at 14° appearing in the latter is due to interferences. The shoulder at 18° of the thin film spectrum might have the same origin. Interference phenomena are very likely reduced in the thin film, because its thickness of 2 unit cells is smaller than the extraction depth of the photoelectrons. Additional differences are expected due to misfit strains and surface relaxation.

3 Discussion

3.1 TiO_2 seed layer

The (110) texture of the TiO_2 film most probably results from the low (110) surface energy. (110) facets of single crystals are by far the most stable ones. For an unrelaxed surface the latter was calculated to be 2.6 N/m, which is considerably less than the second lowest surface energy of 3.7 N/m for (100) facets [20] (both values apply for 0 K). This might be the reason why the (100) orientation is less favorable, in spite of a lower misfit strain in one direction. The epitaxial in-plane orientation for (110) rutile is most probably due to the alignment of the [001] direction with the [1,-1,0] direction of (111) platinum (see Fig. 8). This alignment with an fcc metal has been found before for the opposite situation: Cu films grow epitaxially

with (111) orientation on reconstructed rutile (110) surfaces [21]. In our case, the resulting misfit strains in the rutile are calculated as -7% along [001] and +10% along [-1,1,0].

These values appear to be large. However, this is known to occur for thicknesses that are below the critical value for misfit dislocation formation [22]. The rutile structure with its TiO_2 zig-zag chains (see Fig. 9) running along the (001) direction is possibly rather tolerant for the required modification, since it allows the nearest Ti–O bond length to be unchanged. The Ti–O–Ti angle has only to become smaller, in order to reduce the Ti–Ti distance in the (001) direction. The outwards displacement of the oxygen atoms (rows) has two effects: The in-plane chains elongate the unit cell in the [-1,1,0] direction, as required. The standing chains increase the vertical lattice constant along [110]. A consequence of this chain mechanism would be an increase of the unit cell volume. The results previously obtained by Aoki *et al.* [7] with Ti seed layers deposited in UHV show an optimal thickness of 2 nm Ti for obtaining a good (111) orientation of sol-gel deposited PZT. This is close to our value of 2 nm TiO_2. The Ti film must oxidize completely in air before or during pyrolysis of the PZT sol-gel process. Our experiments with cold and hot deposited TiO_2 allow one to conclude that Aoki's case also consisted of an epitaxial titania film. For the degradation of the seeding effectiveness with larger thick- nesses, three reasons might apply:

1. The TiO_2 layer loses the orientation as soon as bulk energies dominate over surface energies. Thicker films of 100 nm that have been deposited with the same process parameters did indeed exhibit a random orientation of mixed rutile and anatase phases, as observed by x-ray diffraction.
2. The nucleation and transformation of the TiO_2 film to $PbTiO_3$ takes place at almost the same time. With thicker TiO_2 films, a Pb deficiency might occur and lead to transient pyrochlore phases, yielding other orientations.
3. When Ti is used, the oxidation may be incomplete.

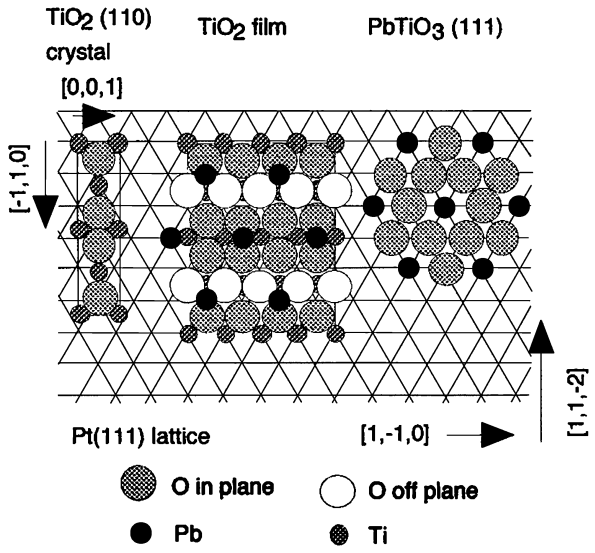

Figure 8. Schematic drawing of TiO_2 rutile (110) on Pt (111). The left part shows the situation with single crystal data. In the center the proposed strained layer is depicted with on top the Pb hexagon of the $PbTiO_3$ (111) orientation. The hexagon of the $PbO_3^{(4-)}$ plane of $PbTiO_3$ is shown on the right hand side.

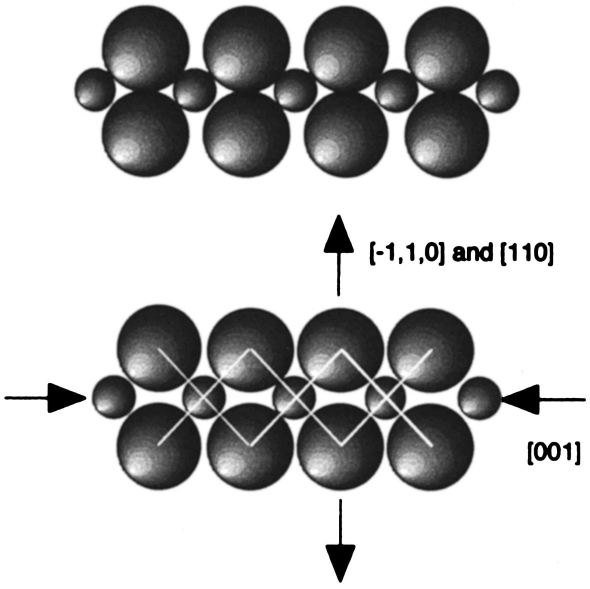

Figure 9. Schematic drawing of a TiO_2 chain. The chains run along the *c* axis and are situated in either the (110) or (1,-1,0) plane. The sizes of the ions have been scaled correctly, using the ion radii published by Shannon and Previtt (see Ref. [32]).

Table I. Calculated polar angles for the shortest bonds in rutile and anatase TiO_2 according to crystal data (Ref. [30]). The orientations with lowest surface energies (according to Ref. [20]) have been selected. The values that would agree with the experiment, i.e. at 0° and between 18° and 25°, are highlighted.

Rutile	Bond length (A)	(110) polar angle	(100) polar angle	
	Ti–Ti 2.96	90°	90°	
	Ti–Ti 3.57	**24.5°**, 90°	49.9°	
	Ti–Ti 4.59	45°	**0°**, 90°	
	Ti–O 1.94	49.4°, 90°	62.8°	
	Ti–O 1.99	**0°**, 90°	45°	
	Ti–O 3.49	**21.3°**, 68.7°	**23.8°**, 66.2°	
	Ti–O 3.56	56.1°, 90°	66.8°	
Anatase	Bond length (A)	(101) polar angle	(100) polar angle	(001) polar angle
	Ti–Ti 3.04	73.2°	51.5°, 90°	38.5°
	Ti–Ti 3.79	**21.7°**, 90°	**0°**, 90°	90°
	Ti–Ti 4.85	**25.1°**, 57.1° 79.5°	38.8°, 67.1°	60,7°
	Ti–O 1.94	34,0°, 85.5°	12.3°, 90°	77.7°
	Ti–O 1.97	68.5°	90°	**0°**
	Ti–O 3.87	43.8°, 79.2°	60.7°	43.8°

3.2 Surface energies and orientational effects in $PbTiO_3$ film growth

It is known that orientation and growth mode in epitaxy are very much determined by the involved interface and surface energies [23]. These depend primarily on the strength and nature of the chemical bonds between film and substrate atoms on the one hand, and between the film atoms on the other hand. Epitaxial relationships lower the interfacial energy. It may occur that the optimal epitaxial relationship does not sufficiently lower the energy, and another orientation may have a more advantageous energy balance due to lower surface energies. Similarly, the orientational effects on bare platinum and on TiO_2 covered platinum can be explained in terms of competing surface and interface energies at the moment of nucleation. With the TiO_2 covered Pt surface (Ti-rich) the interface seems to dominate, in lead rich conditions the surface energy seems to be more important.

Unfortunately, our knowledge of the relevant surface and interface energies is not complete. We nevertheless try to explain the observed behavior with the available data. Platinum exhibits a high surface energy of 2.3 N/m [24,25]. For rutile TiO_2 (110) no experimental values have been found in the literature. A calculated value of 2.6 N/m is reported for the non-relaxed surface [20]. This value seems to be too large in comparison to platinum, because platinum films grow in islands on (110) TiO_2 crystal facets [26] and TiO_2 films, as shown above, completely cover platinum films. Thus the surface energy of TiO_2 should be lower than for Pt, and a value of around 2 N/m seems to be more adequate. We did not find any data for the PbO surface energy. However, a low value can be assumed since the bonding energies are relatively small, (at our deposition conditions for PZT, PbO does not condense to a film but desorbs from the surface), and also because both of the possible bulk structures (tetragonal and orthorhombic) of PbO are layered parallel to the (001) planes. The value may thus be comparable to one for a layered material such as clay (0.31 N/m [25]) or for ones of other oxides such as BaO (0.65 N/m [27]). PbO should therefore have the smallest surface energy of the layers involved. For the sake of surface energy reduction, a PbO coverage of the growing film is therefore advantageous. This behavior was in fact found in the metal system Pb–Ti–Zr, albeit in the absence of oxygen [28].

The interfacial energies of PbO/Pt and TiO_2/Pt determine whether the $PbTiO_3$ film starts with TiO_2, PbO, or a mixture of both on the bare Pt surface. According to our experience, the Pt–O–Ti and Pt–Ti–O interactions are stronger than the Pt–O–Pb and Pt–Pb–O interactions. We observed that the critical flux of PbO for achieving a (100) perovskite nucleation increased with increasing temperature. This means that PbO desorbs considerably from the platinum surface, whereas TiO_2 adheres. A relatively strong interaction

between platinum and (110) rutile is also reported in the literature [26]. Combining the results on surface and interface energies, it is quite reasonable to assume that the lowest energy is acquired by a $PbO/TiO_2/Pt$ monolayer sequence. Since PbO desorbs on PbO, not more than one monolayer of PbO is formed on TiO_2. This layer sequence is the one present in (100) perovskite and will thus preferentially lead to the nucleation of the (100) orientation. As the nuclei are stable and grow further, a low surface energy of the (100) surface must be assumed, or even more, that it has the lowest energy of all the possible surfaces in the presence of excess PbO, which forms a kind of ad-layer on top of the growing film. The above consideration rules out the simple explanation that (100) orientations are due to an epitaxial PbO layer on platinum. Ti has to make the link in any case.

The above argument for the (100) orientation is based on surface and interfacial chemical interactions. The explanation for the growth of (111) PZT needs more subtle arguments, as it results from the weaker interactions of epitaxial ordering. Our experiments showed that a nonoriented or amorphous titania layer failed in seeding the (111) orientation. The ordered surface of the rutile thus plays a significant role. The lead hexagon of the (111) perovskite $PbO_3^{(4-)}$ layer fits indeed well onto a (hypothetical) 4×2 unit cell of the TiO_2 film, as depicted in Fig. 7. Since the strained rutile layer copies the platinum lattice, a very small misfit of 0.5 to $PbTiO_3$ results. It also may be important that the oxygen rows present on the rutile surface work in favor of a $PbO_3^{(4-)}$ coverage, rather than a PbO coverage. The (111) perovskite thus nucleates epitaxially on the TiO_2 seed layer. The smaller grain size of (111) PZT indicates a higher nucleation density, and therefore a smaller activation energy for the nucleation compared to (100) perovskite. For this reason, the (111) orientation may nucleate before the complete coverage with excess PbO has occurred. Afterwards, the seed layer is dissolved in the perovskite. The surface energy of the (111) PZT should not be much larger than that for PZT (100) [29]. The further growth of the (111) orientation is thus maintained, in spite of an excess lead ad-layer. The seeding mechanism described above has not been proposed before. Previous work performed with sol-gel deposition techniques attributed the (111) nucleation to transient phases of either a Pt-Pb alloy [30] or a Pt-Ti alloy [31], which form only in strong reducing conditions. This is not the case in our sputter experiment and can therefore be excluded.

4 Conclusions

In conclusion, it was shown that a crystalline, few nanometer thick TiO_2 film is a very efficient seed layer for the nucleation of PZT (111), working in both, sputter and sol-gel deposition. Growth conditions that lead to $PbTiO_3$ (100) on bare platinum are changed to a (111) orientation if the TiO_2 seed layer is used. XPD measurements show that the latter exhibits a textured microstructure, which most probably corresponds to rutile (110). The epitaxial relationships to the underlying Pt (111) substrate as well as to the $PbTiO_3$ (111) overlayer, together with the lowering of nucleation energy in presence of titania, have been identified to be the driving mechanisms. The occurrence of different textures on bare and on TiO_2 covered Pt (111) surfaces can be explained by competing surface and interface energies.

Acknowledgements

This work was supported by the Swiss Priority Program on Materials. The authors would like to thank K. Schenk from the University of Lausanne for the pole figure measurements, and Jacques Castano for the SEM photographs. Useful discussions with A. Seifert, P. Möckli, and K. G. Brooks are gratefully acknowledged.

References

[1] P. Revesz, J. Li, N. Szabo, Jr., J. W. Mayer, D. Caudillo, and E. R. Myers, Mater. Res. Soc. Symp. Proc. **243**, 101 (1991).

[2] H. N. Al-Shareef, K. D. Gifford, S. H. Rou, P. D. Hren, O. Auciello, and A. I. Kingon, Integrated Ferroelectrics **3**, 321 (1993).

[3] T. Maeder, P. Muralt, L. Sagalowicz, I. Reaney, M. Kohli, A. Kholkin, and N. Setter, Appl. Phys. Lett. **68**, 776 (1996).

[4] R. Ramesh, H. Gilchrist, T. Sands, V. G. Keramidas, R. Haakenaasen, and D. K. Fork, Appl. Phys. Lett. **63**, 3592 (1993).

[5] K. C. Chen and J. D. Mackenzie, Mater. Res. Soc. Symp. Proc. **180**, 663 (1990).

[6] K. G. Brooks, I. M. Reaney, R. D. Klissurska, Y. Huang, L. Bursil, and N. Setter, J. Mater. Res. **9**, 2540 (1994).

[7] K. Aoki, Y. Fukuda, K. Numata, and A. Nishimura, Jpn. J. Appl. Phys., Part 1 **34**, 192 (1995).

[8] K. Sreenivas, I. Reaney, T. Maeder, N. Setter, C. Jagadish, and R. G. Elliman, J. Appl. Phys. **75**, 232 (1994).

[9] G. J. Willems, D. J. Wouters, and H. E. Maes, Microelectron. Eng. **29**, 217 (1995).

[10] G. J. Willems, D. J. Wouters, and H. E. Maes, Integrated Ferroelectrics **15**, 19 (1997).

[11] P. Muralt *et al.*, Proceedings TATF'96, Colmar, April 1-3, 1996, France, Le Vide (Supplément), 1996, pp. 45-47.

[12] M. Kohli, C. Wüthrich, K. Brooks, B. Willing, M. Forster, P. Muralt, N. Setter, and P. Ryser, Sens. Actuators A **60**, 147 (1997).

[13] D. P. Tracy, D. B. Knorr, and K. P. Rodbell, J. Appl. Phys. **76**, 2671 (1994)

[14] T. Maeder and P. Muralt, Mater. Res. Soc. Symp. Proc. **341**, 361 (1994).

[15] T. Maeder, P. Muralt, M. Kohli, A. Kholkin, and N. Setter, Br. Ceram. Proc. **54**, 206 (1995).

[16] J. Osterwalder, T. Gerber, A. Stuck, and L. Schlapbach, Phys. Rev. B **44**, 13764 (1991).

[17] D. Naumovic, A. Stuck, T. Gerber, J. Osterwalder, and L. Schlapbach, Phys. Rev. B **47**, 7462 (1993).

[18] L. Patthey and E. L. Bullock, J. Electron Spectrosc. Relat. Phenom. **83**, 99 (1997).

[19] B. L. Maschhoff, J.-M. Pan, and Th. E. Madey, Surf. Sci. **259**, 190 (1991).

[20] J. Ziolkowksi, Surf. Sci. **209**, 536 (1989).

[21] P. J. Moller and M. C. Wu, Surf. Sci. **224**, 265 □1989□. 22 W. A. Jesser and J. Kui, Mater. Sci. Eng. **164**, 101 (1993).

[22] W. A. Jesser and J. Kui, Mater. Sci. Eng. **164**, 101 (1993).

[23] See, e.g., Jan H. van der Merwe, in *Chemistry and Physics of Solid Surfaces,* Vol II, edited by R. Vanselow (CRC, Boca Raton, FL, 1979).

[24] J. M. Blakely and H. Mykura, Acta Metall. **10**, 565 (1962).

[25] R. G. Linford, in *Solid State Surface Science II,* edited by M. Green (Marcel Dekker, New York, 1973).

[26] Y. M. Sun, D. N. Belton, and J. M. White, J. Phys. Chem. **90**, 5178 (1986).

[27] A. G. Walton, J. Am. Ceram. Soc. **48**, 151 (1965).

[28] O. Auciello, A. R. Krauss, Y. Lin, R. P. H. Chang, and D. M. Gruen, Mater. Res. Soc. Symp. Proc. **341**, 385 (1994).

[29] A. Seifert, A. Vojta, J. S. Speck, and F. F. Lange, J. Mater. Res. **11**, 1470 (1996).

[30] San-Yuan Chen and I-Wei Chen, J. Am. Ceram. Soc. **77**, 2337 (1994).

[31] T. Tani, Z. Xu, and D. Payne, Mater. Res. Soc. Symp. Proc. **310**, 269 (1993).

[32] R. D. Shannon and C. T. Previtt, Acta Cryst. A **32**, 75 (1976).